15. Vincelli, P. C. and Lorbeer, J. W., Forecasting spore episodes of *Botrytis squamosa* in commercial onion fields in New York. *Phytopathology*, 1988, **78**, 966–970.
16. Madden, L., Pennypacker, S. P. and Machnaa, A. A., FAST, a forecast system for *Alternaria solani* on tomato. *Phytopathology*, 1978, **68**, 1354–1358.
17. Dewolf, E. D. and Francl, L. J., Neural network classification of tan spot and stagonespore blotch infection period in wheat field environment. *Phytopathalogy*, 2000, **20**(2), 108–113.
18. Chakraborty, S., Ghosh, R., Ghosh, M., Fernandes, C. D. and Charchar, M. J., Weather-based prediction of anthracnose severity using artificial neural network models. *Plant Pathol.*, 2004, **53**, 375–386.
19. Langenberg, W. J., Sutton, J. C. and Gillespie, T. J., Relation of weather variables and periodicities of airborne spores of *Alternaria dauci*. *Phytopathology*, 1977, **67**, 879–883.
20. Hooker, D. C., Schaafsma, A. W. and Tamburic-Ilincic, L., Using weather variables pre- and post-heading to predict deoxynivalenol content in winter wheat. *Plant Dis*., 2002, **86**, 611–619.
21. Thomas, J., Susela Bhai, R. and Naidu, R., Capsule rot disease of cardamom (*Elettaria Cardamomum* Maton) and its control. *J. Plantation Crops (Suppl.)*, 1991, **18**, 264–268.

ACKNOWLEDGEMENTS. This work was partially supported by a grant from ICRI, Myladumpara and the Network project on Integrated Analysis for Impact, Mitigation and Sustainability, CSIR, New Delhi.

Received 6 May 2014; revised accepted 9 July 2014

Is primary productivity in the Indian Ocean sector of Southern Ocean affected by pigment packaging effect?

S. C. Tripathy*, S. Pavithran, P. Sabu, R. K. Naik, S. B. Noronha, P. V. Bhaskar and N. Anilkumar

National Centre for Antarctic and Ocean Research, Ministry of Earth Sciences, Headland Sada, Vasco-da-Gama, Goa 403 804, India

The probable cause for photoinhibition of primary productivity (PP) in the surface layers of the Indian Ocean sector of the Southern Ocean (SO) was studied during the austral summer (February) 2010. Chlorophyll *a* (Chl *a*) and PP values were higher for polar stations compared to offshore stations and showed surface maxima; however, subsurface Chl *a* maxima was observed in two of the offshore stations. Biomass explained 36% of variance in PP and was not the sole controlling factor for PP variability. Euphotic zone integrated PP showed increasing trend from offshore to polar stations and varied from 159.56 to 1083.57 mg C m^{-2} d^{-1}. The relationship between Chl *a*-specific PP (P^B) and the corresponding photosynthetically active radiation in the water column was linear for offshore and curvilinear for polar stations, indicating the occurrence of 'photoinhibition' in the surface waters of polar stations. This could be ascribed to the onset of pigment packaging (the 'package effect') as larger phytoplankton (diatoms) dominated the polar stations, where macronutrients ratio was ideal (N : P ~ 16 and N : Si ~ 1) for growth of diatoms. Despite high Chl *a* in the polar waters, the corresponding PP was proportionally not high compared to the offshore stations. We suggest that larger phytoplankton are susceptible to pigment packaging, which in turn decreases their light-absorption/photosynthetic efficiency, resulting in lower PP, which is otherwise expected to be higher in the presence of elevated biomass.

Keywords: Light absorption, package effect, primary productivity, phytoplankton community.

THE Southern Ocean (SO) is potentially one of the most productive regions in the World's Oceans, considering the concentration of macronutrients (especially NO_3) it retains in the surface layers. Nevertheless, it is characterized by low primary productivity (PP) or high-nutrient low-chlorophyll (HNLC) phenomenon. The candidate mechanisms suggested to control the magnitude of PP in this HNLC ecosystem include fluctuating light levels, low iron supply, silicic acid concentration, high grazing pressure and low water temperature[1]. PP plays a significant role in drawdown of atmospheric CO_2 and transports it to the ocean interior through 'biological pump'. Thus, it is imperative to have a clear understanding of the cause(s) responsible for PP variability in the SO. PP in nutrient-rich waters is a function of three basic variables: chlorophyll *a* (Chl *a*), photosynthetically active radiation (PAR) availability, and light absorption capacity (Chl *a*-specific absorption coefficient)[2]. Beside this, PP also depends on another photo-physiological property of the phytoplankton, the efficiency with which the microscopic plants are able to convert the absorbed PAR into carbon (i.e. the quantum yield of carbon fixation). The light absorption capacity and the quantum yield of carbon fixation have been reported to be dependent on the phytoplankton community composition[3,4]. The light-absorbing efficiencies of phytoplankton communities directly regulate PP and are the major biological determinant of *in situ* subsurface light field in case I waters[5,6].

In oceanic environment, shifts in the hydrological parameters drive the changes in phytoplankton composition and their mean cell size[7,8], and hence, influence the internal accumulation of pigments and their packaging degree[9,10]. Thus, hydrological alterations affect the light-absorption/photosynthetic efficiency of phytoplankton communities. The 'package effect' (i.e. loss of linearity between light-harvesting efficiency and pigment packaging) originates from intracellular shading of the chloroplasts

*For correspondence. (e-mail: sarat@ncaor.gov.in)

on one another. In general, when Chl *a* increases, cell size also increases[11]. Increase in pigment density within a cell or increase in cell size of a population results in increased pigment packaging thereby decreasing the light-absorption/photosynthetic efficiency along with decrease in P^B or assimilation number[12]. Large/micro phytoplankton generates a strong packaging effect (package effect becomes significant for cell sizes >10 μm), producing low Chl *a*-specific absorption, conversely the package effect in small phytoplankton is less and results in relatively high Chl *a*-specific absorption[11]. Thus, if Chl *a* increases in a particular region, we would see a decrease in Chl *a*-specific PP (P^B) if package effect is playing a role[12]. The package effect and pigment composition are suggested as the major factors causing the variability in absorption properties of phytoplankton[13]. These two factors are different among and within phytoplankton populations growing under various environmental conditions (e.g. nutrient and irradiance levels)[11].

In SO, especially the region between the polar front and coastal Antarctica (henceforth, polar waters) is usually characterized by large cell species, i.e. diatoms. For SO, the importance of pigment packaging has been known for sometime[12,14], however, its relationship to PP in the Indian Ocean sector of the SO has not been previously appreciated. The optical properties of coastal waters are complex due to the prevailing dynamic hydrographic conditions (e.g. freshwater intrusion, upwelling and mixing)[15]. Studies have shown that freshwater intrusion could significantly change the light-absorption budget among phytoplankton, detritus and coloured dissolved organic matter[15,16]. During austral summer, the polar waters (south of 60°S) of SO, is significantly influenced by meltwater intrusion from the Antarctic ice shelf[17]. Thus, the nutrient-rich (NO_3, SiO_4 and Fe) freshwater mixes with the surrounding high saline waters and spreads offshore. It has been observed that the meltwater intrusion enhances Chl *a*, resulting in high PP in the upper layer of the SO[18]. The phytoplankton community has also been reported to be modulated by the meltwater. Therefore, it is likely to have an influence on phytoplankton light-absorption properties in the SO, especially in the surface layer. Hence, it is important to assess the influence of package effect on P^B because the latter is significantly affected by the former. However, knowledge on this aspect is scanty in the Indian Ocean sector of the SO. Therefore, the present study aims to investigate whether photoinhibition is affecting PP variability, and also the causative factors for the variability in PP between the polar and offshore regions in the Indian Ocean sector of the SO.

Water samples were collected for analysis of physico-chemical and biological variables at six stations (Figure 1) along the meridional transect (57°30′E) from 44°S to 65°32′S on-board *ORV Sagar Nidhi* during the austral summer (February) 2010 (Table 1). Vertical profiles of temperature (°C) and salinity were measured by CTD (SBE 911+, USA). Intensity of PAR in the water column was measured by a PAR sensor (QSP-2200, Biospherical) attached to the CTD-rosette (General Oceanic Inc.). The vertical attenuation coefficient for downwelling PAR (K_d) was calculated by regression fit of the vertical underwater light profiles. Sea-surface temperature (SST; ±0.2°C) was measured using a bucket thermometer (Theodor Friedrichs & Co, Germany). Water sampling from standard depths (0, 10, 30, 50, 70, 100 and 120 m) was carried out using Niskin bottles attached to a rosette sampler. Inorganic macronutrients (NO_3, SiO_4 and PO_4) were estimated spectrophotometrically, whereas dissolved oxygen (DO) was estimated by the Winkler method using standard protocols[19]. Surface PAR (μE m^{-2} s^{-1}) was calculated from the automatic weather station (AWS) situated on-board the vessel and integrated over the photoperiod to get daily incident PAR (E m^{-2} d^{-1}). Chl *a* was measured spectrophotometrically[19]. Chl *a* (mg m^{-3}) values at different depths were integrated to obtain column Chl *a* (mg m^{-2}).

Simulated *in situ* on-deck incubation experiments were carried out to quantify ^{14}C-based PP from five depths (0, 30, 50, 70 and 120 m) covering the euphotic depth (Z_{eu}, where 1% incident PAR level is attained). Detailed description of the methodology used for this incubation is mentioned elsewhere[19,20]. Daily PP rates (mg C m^{-3} d^{-1}) at discrete depths were trapezoidally integrated to estimate the euphotic zone-integrated PP (IPP, mg C m^{-2} d^{-1}).

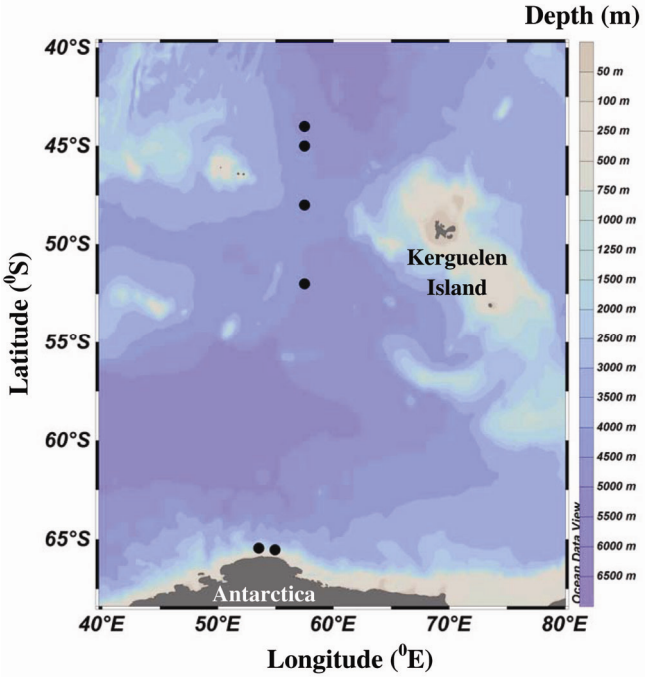

Figure 1. Station locations (filled dots) in the Indian Ocean sector of the Southern Ocean. The two stations near the Antarctica landmass and the four stations north of 53°S are considered as polar and offshore stations respectively.

Table 1. Latitude, longitude, sea surface temperature (SST), sea surface salinity (SSS), surface nutrients (NO_3, SiO_4, PO_4), water column average N : P and N : Si ratios, surface dissolved oxygen (DO), surface photosynthetically active radiation (PAR), surface chlorophyll *a* (Chl_0), column-integrated chlorophyll *a* (Chl_{int}), surface primary productivity (Sur. PP), column-integrated PP (IPP), and surface Chl *a*-specific PP (P^B) at different stations

Station no.	Latitude (°S)	Longitude (°E)	SST (°C)	SSS	NO_3 (μM)	SiO_4 (μM)	PO_4 (μM)	N : P	N : Si	DO (ml l^{-1})	PAR (E m^{-2} d^{-1})	Chl_0 (mg m^{-3})	Chl_{int} (mg m^{-2})	Sur. PP (mgC m^{-3} d^{-1})	IPP (mgC m^{-2} d^{-1})	P^B (mgC (mgChl *a*)$^{-1}$ d^{-1})
1	44°00′	57°30′	12.47	34.13	13.70	1.54	1.03	14.21 + 0.76	8.98 + 2.98	6.17	46.58	0.53	38.73	2.90	159.57	5.43
2	45°00′	57°30′	11.11	33.89	20.80	1.44	1.41	13.48 + 1.87	9.99 + 3.21	6.19	17.45	0.40	53.10	4.57	201.50	11.50
3	48°00′	57°30′	8.47	33.72	24.33	3.08	1.63	14.05 + 3.32	5.90 + 1.63	6.51	26.88	0.10	9.13	4.25	288.20	40.70
4	52°00′	57°30′	4.45	33.85	34.16	10.21	2.01	16.29 + 0.91	2.18 + 0.66	7.20	24.28	0.36	52.50	2.61	167.02	7.22
5	65°27′	53°32′	–0.61	33.70	37.37	82.26	2.54	15.61 + 2.59	0.51 + 0.08	8.03	36.36	4.10	265.63	7.90	397.15	1.92
6	65°32′	54°56′	–0.43	33.56	29.13	67.82	2.17	13.25 + 1.21	0.48 + 0.04	8.05	26.72	3.15	183.75	19.83	1083.5	6.30

Furthermore, PP values at discrete depths were normalized to the corresponding Chl *a* to calculate P^B (mg C (mg Chl *a*)$^{-1}$ d^{-1}) or the assimilation number, which is an indictor of the phytoplankton adaptation to the ambient environment.

The relationship between P^B and the corresponding underwater PAR (henceforth, PAR–P^B relationship) was obtained by curve-fitting method. In this study, the PAR–P^B relationship does not correspond to the true photosynthesis–irradiance (P–E) response of the same phytoplankton assemblages; rather, it represents the relationship between P^B and the corresponding PAR at different depths in the water column. And it can similarly be described as P–E response[21]. For curve fitting, the P–E model[22] containing only two photosynthetic parameters was used, which can be described by the following equation

$$P^B = P^B_{opt} (E/E_{max}) - \exp [1 - (E/E_{max})], \quad (1)$$

where P^B, P^B_{opt} and E_{max} are Chl *a*-normalized carbon fixation rate (mg C (mg Chl *a*)$^{-1}$ h^{-1}), Chl *a*-normalized optimal carbon fixation rate (mg C (mg Chl *a*)$^{-1}$ h^{-1}) in the water column, and irradiance value at the point of inflection between light-limited and light-saturated phases (μE m^{-2} s^{-1}) respectively

$$P^B = P^B_{opt}[1 - \exp (-E/E_{max})]. \quad (2)$$

When no photoinhibition was apparent, the model of Webb *et al.*[23] was fitted (eq. (2)) to the dataset to retrieve the photosynthetic parameters. The parameter definitions in eq. (2) are same as eq. (1).

Water column (up to 120 m) temperature and salinity varied from –1.43°C to 12.47°C (avg 5.04 ± 4.80°C) and 33.55 to 34.60 (avg 33.95 ± 0.23) respectively. SST and sea-surface salinity (SSS) ranged from –0.60°C to 12.47°C (avg 5.91 ± 5.68°C) and 33.56 to 34.13 (avg 33.81 ± 0.19) respectively. A decreasing trend in SST and SSS towards the south was observed along the meridional transect (Table 1). SST decreased by ~1.0°C per degree latitude between 44°S and 52°S. SST in the polar stations was below 0°C and was accompanied by comparatively low saline waters. Unlike in SST, the decreasing trend in salinity was not sharp from north to south (Table 1). The polar stations showed large salinity gradient in the water column with decreasing salinity values towards the surface, which could be due to the influence of meltwater originated from the glacial ice resulting in a buoyant layer of comparatively low-saline surface waters varying in temperature between –0.60°C and –0.43°C (ref. 24). Surface dissolved oxygen (DO; ml l^{-1}) showed a distinct increasing trend towards the Antarctica coast and reached as high as 8.05 ml l^{-1} (Table 1). Surface DO was inversely correlated with both SST ($r^2 = 0.99$) and SSS ($r^2 = 0.60$). The vertical attenuation coefficient for downwelling PAR (K_d) varied from 0.05 to 0.09 m^{-1} and the depth of the euphotic zone (Z_{eu}) was between 55 and 85 m during the study period. Higher K_d values and therefore shallower euphotic depths occurred in the polar stations. Vertical light attenuation was higher in the presence of higher biomass, which could be discerned as the K_d values were strongly related ($r^2 = 0.61$) to Z_{eu}-integrated (henceforth, column-integrated) Chl *a* concentrations, indicating that Chl *a* had strong contribution for the vertical attenuation of the incident PAR. Mixed layer depth (MLD) was shallower than Z_{eu} at all stations, which is in accordance with an earlier report[25]. Z_{eu} > MLD indicates the favourable light availability for PP. The daily integrated incident PAR varied from 17.45 to 46.58 E m^{-2} d^{-1} (Table 1). The average PAR value was moderately high (29.71 + 10.25 E m^{-2} d^{-1}) during the study period and hence may not have been a limiting effect for phytoplankton growth. PAR values did not show any clear latitudinal variation. The low PAR value (17.45 E m^{-2} d^{-1}) at 45°S could be ascribed to the varying cloudiness. The day length increased southwards from 14:20 to 15:30 h, which is consistent with those previously recorded for this sector of the SO[26].

In general, the macronutrients (NO_3, PO_4 and SiO_4) increased southward and with depth. Although NO_3 and PO_4 in the surface layer were consistently high (NO_3: 13.70–37.37; avg 26.85 ± 8.76 μM), PO_4 (1.03–2.54; avg 1.79 ± 0.55 μM), SiO_4 concentration (1.44–82.26; avg 27.72 ± 37.07 μM) differed markedly from north to south, with very high values in the polar stations (Figure 2 *a*). Low SiO_4 concentration (1.54–10.21 μM) was observed north of the Polar Front (PF), including the PF (henceforth, offshore stations, i.e. 44°–52°S), whereas high concentrations (67.82–82.27 μM) were found south of the PF, i.e. close to the Antarctic coast (beyond 65°S). Our results are in good agreement with earlier findings[27], which indicate that approximately half the area of the SO (the sub-Antarctic zone) is SiO_4-poor year round. SiO_4 is an essential nutrient for diatoms, and the strong SiO_4 gradient observed across the meridional transect suggests that large diatoms (> 10 μm) may dominate the phytoplankton population south of the PF, whereas nonsiliceous species would dominate in waters north of the PF[28,29]. Both Fe- and Zn-limited diatoms have reduced abilities to compete for SiO_4 and hence, the low SiO_4 concentrations in the sub-Antarctic waters would prevent diatoms from consuming more than 5% of the available NO_3, thereby causing hindrance to their growth[29]. Redfield *et al.*[30] have highlighted the importance of N, P and Si, which potentially regulate phytoplankton biomass and showed that when the nutrient concentrations are adequate for healthy growth of diatoms, the atomic N : P : Si ratio within the cells is about 16 : 1 : 16. Subsequently, other studies[31,32] have shown that ambient N : P < 10 and N : Si < 1 could be indicative of a potential N-limitation, whereas N : Si > 1 and Si : P < 3 are indicative of

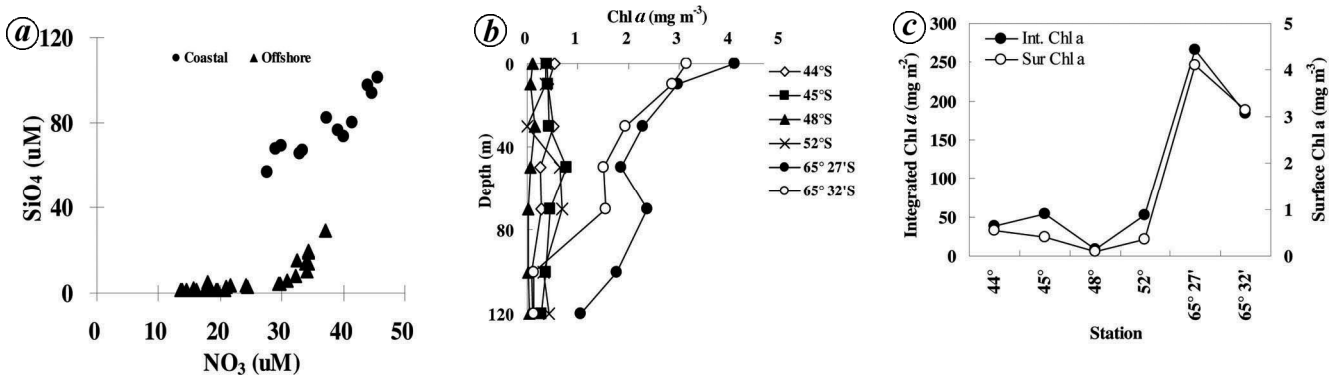

Figure 2. ***a***, Scatter plot of silicate and nitrate; ***b***, Vertical profiles of Chl *a*; ***c***, Line plot of surface and column-integrated Chl *a* in the study area.

Si-limitation[33]. Also, deviation from the Redfield ratio can create an ambience suitable for the growth of smaller phytoplankton (nano and pico; as they are more competitive at high N : P ratios with low P), as reported elsewhere[34]. During our observation, surface-layer N : P ratio was more or less consistent (13.30–17.01), nearing the Redfield ratio, throughout the study area (Table 1), whereas the N : Si ratio was far higher than the Redfield ratio in the offshore waters, which indicates that SiO_4 is highly limiting (surface SiO_4 concentration <5.0 μm) to diatoms and/or silicoflagellates growth[28]. The observed Si-limitation in the offshore could be due to the preferential removal of silicic acid generally attributed to the influence of Fe-limitation[35]. Conversely, the N : Si ratio approached (0.48–0.51) the Redfield ratio in the polar stations, indicating that the prevailing ambience in the polar waters was ideal for larger phytoplankton (diatoms) growth. It has been reported earlier that the region south of the Antarctic Circumpolar Current (ACC) creates a favourable environment for growth of diatoms/silicoflagellates[28]. During this study, the low PP recorded in the offshore waters could partially be attributed to the Si-limitation[35].

Considering the proximity to Antarctic landmass, Fe-limitation in the polar waters may not be as severe as in the offshore stations, where low Fe concentrations are known to favour the growth of small cells[36]. Since Fe uptake by phytoplankton varies with cell surface to volume ratio, small phytoplankton (mainly pico-sized) may grow faster when ambient Fe concentrations are low[37]. Low Fe combined with low SiO_4 availability in the offshore region has been shown to support the growth of nonsiliceous, iron-efficient phytoplankton species such as pico-phytoplankton and cyanobacteria[38]. Upon Fe-enrichment, the larger phytoplankton (predominantly diatoms) become dominant as their population density cannot be regulated by microzooplankton grazing due to their large size and higher growth rates than their grazers[1].

During the study period surface Chl *a* concentration varied from 0.10 to 4.10 (0.87 ± 0.98) mg m^{-3} and was within the reported range as in most of the SO[18]; the mean Chl *a* concentrations remains quite low (0.3–0.4 mg m^{-3}) and rarely exceed 0.6 mg m^{-3}. Chl *a* concentration was lower in the offshore stations compared to the polar stations (Figure 2 *b*), with subsurface Chl *a* maximum (SCM) for two offshore stations (45°S and 52°S) at ~50 and 70 m depth. Surface Chl *a* concentration seemed to be associated with temperature and salinity distribution, with enhanced biomass coinciding with cooler and fresher waters and vice versa. The column-integrated Chl *a* and surface Chl *a* were higher for the polar stations compared to offshore stations (Table 1 and Figure 2 *c*), implying that surface Chl *a* has a strong contribution in the column-integrated Chl *a*. Thus, it can be inferred that the surface layer productivity is expected to play a crucial role in determining the column-integrated productivity. Earlier reports have shown that integrated Chl *a* in the SO was very high in diatoms dominant waters[24,39], which influenced the vertical light penetration. The observed high integrated Chl *a* in the polar waters could have substantially reduced the light penetration, thereby resulting in the shallowest euphotic zone in the entire study area.

The surface PP ranged between 2.61 and 19.83 (7.01 ± 6.55) mg C m^{-3} d^{-1} and like Chl *a* did not show any clear trend from north to south (Figure 3 *a*, Table 1). The PP values for polar stations were higher than that of the offshore stations. Vertical profiles of PP showed clear subsurface maxima at ~30 m (Figure 3 *a*), which did not coincide with the SCM depths (Figure 2 *b*). Regression analysis ($r^2 = 0.36$) between Chl *a* at discrete depths and corresponding PP (Figure 3 *b*) showed that only 36% of the variance in PP could be explained by biomass, indicating that Chl *a* may not be the sole controlling factor for PP variability during the study period. IPP ranged (Table 1) from 159.56 to 1083.56 (382.80 ± 354.84 mg C m^{-2} d^{-1}). The production rates measured in this region are within the range of previous measurements carried out in the SO during the austral summer[25,26].

The surface P^B varied from 1.92 to 40.70 mg C (mg Chl *a*)$^{-1}$ d^{-1} (Figure 4 *a*). In the water column, the range and average of P^B for offshore stations (0.23–11.50; avg 4.00 ± 3.08; station 48°S was excluded from this

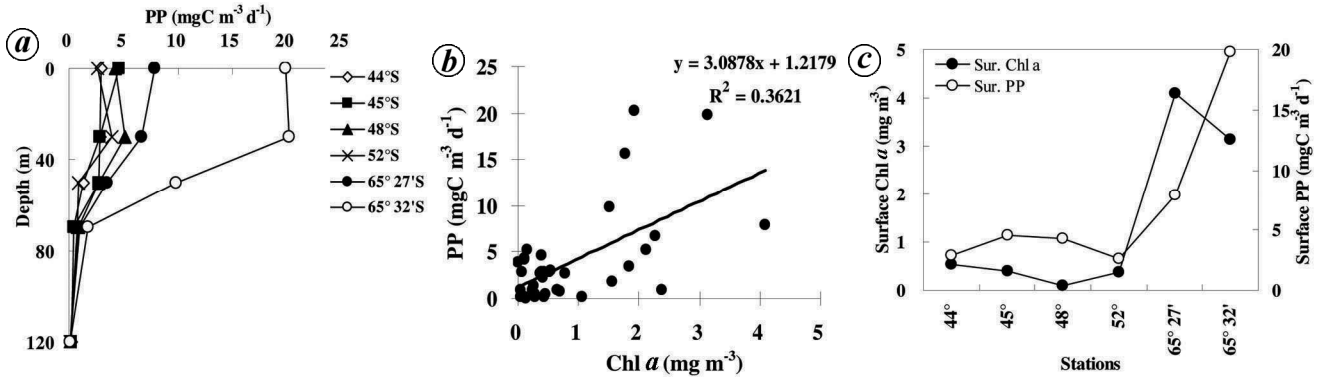

Figure 3. ***a***, Vertical profiles of primary productivity (PP); ***b***, Scatter plot of Chl *a* and PP at discrete depths; ***c***, Line diagram of surface Chl *a* and PP in the study area.

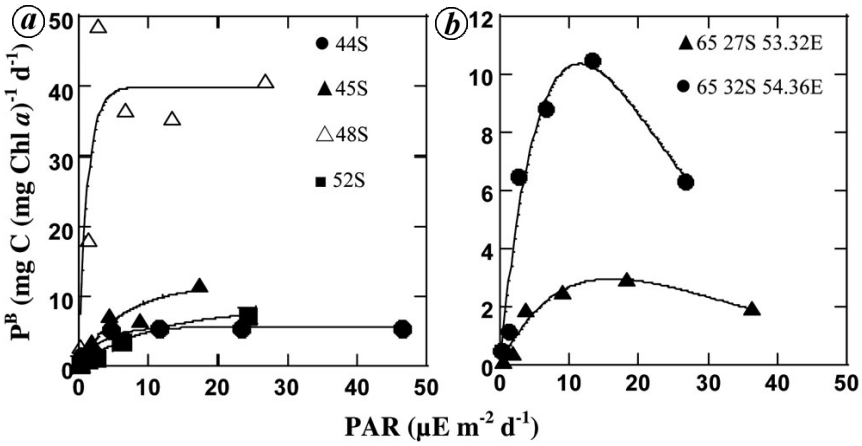

Figure 4. Daily photosynthetically active radiation (PAR)–P^B relationships in the water column for (***a***) offshore (along 57°30′E) and (***b***) polar stations.

calculation, which is discussed later in the text) were slightly higher than that of the polar stations (0.10–10.47; avg 3.60 ± 3.51), implying that the offshore phytoplankton cells were relatively more photosynthetically efficient than the polar water phytoplankton, allowing higher production rates (P^B) despite having lower biomass and similar intensity of incident PAR. The PAR–P^B relationship was linear and curvilinear for the offshore and polar stations respectively. Unlike offshore stations (Figure 4 *a*), decrease of P^B in the surface layer (hereafter, photoinhibition) was observed for the polar stations (Figure 4 *b*) at similar intensities of incident PAR (Figure 4 *a* and *b*). No clear trend was observed between surface Chl *a* and corresponding PP (Figure 3 *c*). Nevertheless, the increase in surface PP with respect to the increase in surface Chl *a* at the polar station (Stn 5, Table 1) was proportionately low compared to the offshore stations, which could be mainly due to the lower P^B in the surface layer associated with the onset of pigment packaging. Though the other polar station (Stn 6) depicted proportionate increase in PP with respect to Chl *a*, it could have been even higher had there been no decline in surface layer P^B. Earlier reports[40,41] had attributed the commonly found high Chl *a* and low assimilation numbers in the SO to the pigment packaging and community structure, which corroborates our findings.

Phytoplankton cells are known to respond to variability of light intensity in order to protect the photosynthetic process from photo-damage. In general, decrease in phytoplankton absorption occurs with an increase in Chl *a*[11]. Thus, if Chl *a* increases in a particular region, we would see a decrease in P^B if package effect is playing a role[12]. During austral summer, the coastal area off Antarctica is influenced by the intrusion of meltwater containing very high concentrations of NO_3, SiO_4 and Fe[42]. The low saline waters (< 33.5) observed in the polar stations may have originated from the Antarctic continent as a result of melting of glacial ice and/or snow, which is commonly seen along the continental shelf of Antarctica during late summer to early fall (January–March). It has been suggested that the meltwater enhances Chl *a*, resulting in high PP in the upper layer off costal Antarctica[18]. The phytoplankton community has also been reported to be modulated by meltwater[43]. Consequently, the meltwater is expected to influence the phytoplankton light-absorption properties of the coastal Antarctica, especially in the surface layer.

In the present context, the photoinhibition effect is indicative of probable occurrence of different phytoplankton community structure or the available incident PAR. From the *in situ* measurements of daily integrated PAR, it can be concluded that there was no marked difference between the light regime of offshore and polar stations. Hence, the role of the incident PAR for the observed photoinhibition (decreasing surface P^B in polar stations) could be negligible. The maximum P^B values for both offshore (Figure 4 *a*) and polar (Figure 4 *b*) stations were close to ~10 mg C (mg Chl *a*)$^{-1}$ d^{-1}, with an exception at 48°S, where the vertical Chl *a* concentrations were lowest compared to the other offshore stations; however, the corresponding PP values were high, thereby resulting in disproportionately (four times) higher P^B compared to the other offshore stations. This decoupling between Chl *a* concentrations and PP could be due to the existence of an entirely different phytoplankton population (pico-phytoplankton can enhance PP without causing a large increase in biomass) than that of other offshore stations. Westwood *et al.*[41] have observed assimilation numbers as high as 75 mg C (mg Chl *a*)$^{-1}$ d^{-1} corresponding with high abundance of nanoflagellates, as well as autotrophic dinoflagellates in the sub-Antarctic zone (around 48°S) off Tasmania. These groups do not require SiO_4 for growth and are likely to contribute to efficient photosynthesis in the surface layer[41]. From nutrient data it is evident that offshore stations, including 48°S were severely limited with SiO_4 and hence unfavourable for growth of large/micro phytoplankton (diatoms). Consequently, this condition might have been conducive for the smaller phytoplankton (flagellates, nano- and pico-sized) to grow because of their high surface to volume ratio, which enables them to utilize the minimal available macronutrients more efficiently. This canonical hypothesis could be supported by the diagnostic pigment (DP) analysis. Phytoplankton pigment samples for HPLC analyses were not collected for this period; however, the DP analysis from the subsequent year (2012) in this region (unpublished) shows that the offshore stations were dominated by nanoflagellates (92%) followed by diatoms (7%) and prokaryotes (1%). On the contrary, the polar stations were dominated by diatoms (59%) followed by flagellates (40%) and prokaryotes (1%). These results support the preference of community structure based on availability of nutrients. Previous documentations show the dominance of nano- and pico-phytoplankton and diatoms in the north and south of the PF zone respectively[28,44].

The SO is known for its characteristic HNLC condition. Low productivity in different zones of the SO has been ascribed to deep mixing-induced light limitation, grazing pressure, limitations of maximum photosynthetic efficiency by low water temperatures, and trace metal limitation. For the SO, the significance of phytoplankton pigment packaging has been recognized for some time; however, its relationship to PP in the Indian sector of the SO has not been previously appreciated. Datasets collected from the Indian Ocean sector of the SO during the austral summer of 2010 were used to address the effect of pigment packaging in reducing the magnitude of PP, especially in the surface layer. Our analysis shows that in the presence of favourable nutrient conditions, at similar intensities of incident light, the Chl-*a* specific PP in the surface layer decreased for the polar stations, whereas no such decrease was observed for offshore stations. Decrease in Chl-*a* specific PP in the surface layer is hypothesized to be due to the onset of pigment packaging effect, which is pronounced in large/micro phytoplankton (diatoms) compared to the nano/pico-sized one. Column-integrated Chl *a* and PP for polar stations were significantly higher than the offshore stations, which could be attributed to the predominance of diatoms in the polar stations. The nutrient ratios (N : P and N : Si) were close to the Redfield ratio in the polar area. As the polar stations are in the proximity of the Antarctica landmass, abundance of macronutrients/trace metals along with the ideal nutrient ratios could have sustained the growth of diatoms. Conversely, in the offshore regions deviation from the ideal Redfield ratio, and preferential uptake of SiO_4 in conjunction with trace metal limitation sustained the growth of smaller phytoplankton (nano and pico), as reflected through the diagnostic pigment analysis. Specifically, the N : Si ratio seems to influence the phytoplankton community structure in the study area. Our findings suggest that even though the Chl *a* concentration was very high in the polar waters, the corresponding PP values were proportionally not very high compared to the offshore stations. This is because the larger/micro phytoplankton are susceptible to pigment packaging, which in turn decreases their light-absorption or photosynthetic efficiency, thereby reducing the magnitude of IPP, which is otherwise expected to be higher in the presence of elevated biomass. Detailed studies need to be carried out to re-establish the effect of package effect and its relationship to the PP variability in this region of the SO.

1. De Baar, H. J. W. and Boyd, P. W., The role of iron in plankton ecology and carbon dioxide transfer of the global oceans. In *The Changing Ocean Carbon Cycle: A Midterm Synthesis of the Joint Global Ocean Flux Study* (eds Hanson, R. B., Ducklow, H. W. and Field, J. G.), Cambridge University Press, 2000, pp. 61–140.
2. Behrenfeld, M. J. and Falkowski, P. G., A consumer's guide to phytoplankton primary productivity models. *Limnol. Oceanogr.*, 1997, **42**, 1479–1491.
3. Ciotti, A. M., Cullen, J. J. and Lewis, M. R., A semi-analytical model of the influence of phytoplankton community structure on the relationship between light attenuation and ocean color. *J. Geophys. Res.*, 1999, **104**(C1), 1559–1578.
4. Claustre, H. *et al.*, Towards a taxon-specific parameterization of bio-optical models of primary production: a case study in the North Atlantic. *J. Geophys. Res.*, 2005, **110**, 1–17.
5. Smith, R. C. and Baker, K. S., The bio-optical state of ocean waters and remote sensing. *Limnol. Oceanogr.*, 1978, **23**, 247–259.
6. Morel, A., Optical modeling of the upper ocean in relation to its biogenous matter content (case I waters). *J. Geophys. Res.*, 1988, **93**, 10749–10768.

7. Margalef, R., Life-forms of phytoplankton as survival alternatives in an unstable environment. *Ocean. Acta*, 1978, **1**, 493–509.
8. Yentsch, C. S. and Phinney, D. A., A bridge between ocean optics and microbial ecology. *Limnol. Oceanogr*., 1989, **34**, 1694–1705.
9. Alalli, K., Bricaud, A. and Claustre, H., Spatial variations in the chlorophyll-specific absorption coefficients of phytoplankton and photosynthetically active pigments in the equatorial Pacific. *J. Geophys. Res*., 1997, **102**, 12413–12423.
10. Vidussi, F., Claustre, H., Manca, B., Luchetta, A. and Marty, J. C., Phytoplankton pigment distribution in relation to upper thermocline circulation in the eastern Mediterranean Sea during winter. *J. Geophys. Res*., 2001, **106**, 19939–19956.
11. Bricaud, A., Babin, M., Morel, A. and Claustre, H., Variability in the chlorophyll-specific absorption coefficients for natural phytoplankton: analysis and parameterization. *J. Geophys. Res*., 1995, **100**, 13321–13332.
12. Marra, J., Trees, C. C. and O'Reilly, J. E., Phytoplankton pigment absorption: a strong predictor of primary productivity in the surface ocean. *Deep-Sea Res. I*, 2007, **54**, 155–163.
13. Lohrenz, S. E., Weidemann, A. D. and Tuel, M., Phytoplankton spectral absorption as influenced by community size structure and pigment composition. *J. Plankton Res*., 2003, **25**, 35–61.
14. Mitchell, B. G. and Holm-Hansen, O., Bio-optical properties of Antarctic peninsula waters: differentiation from temperate ocean models. *Deep-Sea Res.*, 1991, **38**, 1009–1028.
15. Babin, M., Stramski, D., Ferrari, G. M., Claustre, H., Bricaud, A., Obolensky, G. and Hoepffner, N., Variations in the light absorption coefficients of phytoplankton, non-algal particles, and dissolved organic matter in coastal waters around Europe. *J. Geophys. Res*., 2003, **108**, 3211; doi:10.1029/2001jc000882.
16. Brunelle, C. B., Larouche, P. and Gosselin, M., Variability of phytoplankton light absorption in Canadian Arctic seas. *J. Geophys. Res*., 2012, **117**, C00G17; doi:10.1029/2011jc007345.
17. Dierssen, H. M., Smith, R. C. and Vernet, M., Glacial meltwater dynamics in coastal waters west of the Antarctic peninsula. *Proc. Natl. Acad. Sci. USA*, 2002, **99**(4), 1790–1795.
18. Moore, J. K. and Abbott, M. R., Phytoplankton chlorophyll distributions and primary production in the Southern Ocean. *J. Geophys. Res*., 2000, **105**, 28709–28722.
19. Strickland, J. D. H. and Parsons, T. R., A practical handbook of seawater analysis. *J. Fish. Res. Board. Can.*, 1972, **167**, 310.
20. Pavithran, S. *et al*., Contrasting pattern in chlorophyll *a* distribution within the Polar Front of the Indian sector of Southern Ocean during austral summer 2010. *Curr. Sci.*, 2012, **102**(6), 899–903.
21. Sakshaug, E. *et al*., Parameters of photosynthesis: definitions, theory and interpretation of results. *J. Plankton Res.*, 1997, **19**, 1637–1670.
22. Steele, J. H., Environmental control of photosynthesis in the sea. *Limnol. Oceanogr.*, 1962, **7**, 137–149.
23. Webb, W. L., Newton, M. and Starr, D., Carbon dioxide exchange of *Alnus rubra*: a mathematical model. *Oecologia*, 1974, **17**, 281–291.
24. Valliancourt, R. D., Sambrotto, R. N., Green, S. and Matsuda, A., Phytoplankton biomass and photosynthetic competency in the summertime Mertz Glacier Region of East Antarctica. *Deep-Sea Res. II*, 2003, **50**, 1415–1440.
25. Gandhi, N. *et al.*, Zonal variability in primary production and nitrogen uptake rates in the southwestern Indian Ocean and the Southern Ocean. *Deep-Sea Res. I*, 2012, **67**, 32–43.
26. Jasmine, P. *et al.*, Hydrographic and productivity characteristics along 45°E longitude in the southwestern Indian Ocean and Southern Ocean during austral summer. *Mar. Ecol. Prog. Ser.*, 2009, **389**, 97–116.
27. Trull, T. *et al.*, Circulation and seasonal evolution of polar waters south of Australia: implications for iron fertilization of the Southern Ocean. *Deep-Sea Res. II*, 2001, **48**, 2439–2466.
28. Franck, V. M., Brzesinski, M. A., Coale, K. H. and Nelson, D. M., Iron and silicic acid concentrations regulate Si uptake north and south of the Polar Frontal Zone in the Pacific Sector of the Southern Ocean. *Deep-Sea Res. II*, 2000, **47**, 3315–3338.
29. Coale, K. H., Southern Ocean iron Enrichment Experiment: carbon cycling in high and low-Si waters. *Science*, 2004, **304**, 408–414.
30. Redfield, A. C., Ketchum, B. H. and Richards, A., The influence of organisms on the composition of sea water. In *The Sea* (ed. Hill, M. M.), Interscience, New York, 1963, vol. 2, pp. 26–77.
31. Brzezinski, M. A., The Si : C : N ratio of marine diatoms: interspecific variability and the effect of some environmental variables. *J. Phycol.*, 1985, **21**, 347–357.
32. Levasseur, M. E. and Therriault, J. C., Phytoplankton biomass and nutrient dynamics in a tidally induced upwelling: the role of NO_3 : SiO_4 ratio. *Mar. Ecol. Prog. Ser*., 1987, **39**, 87–97.
33. Harrison, P. J., Conway, H. L., Holmes, R. W. and Davis, C. O., Marine diatoms in chemostats under silicate or ammonium limitation. III. Cellular chemical composition and morphology of three diatoms. *Mar. Biol.*, 1977, **43**, 19–31.
34. Mackey, K. R. M. *et al.*, Aerosol-nutrient-induced picoplankton growth in Lake Tahoe. *J. Geophys. Res.*, 2013, **118**, 1–14.
35. Sarmiento, J. L., Gruber, N., Brzezinski, M. A. and Dunne, J. P., High-latitude controls of thermocline nutrients and low latitude biological productivity. *Nature*, 2004, **427**, 56–60.
36. Timmermans, K. R. *et al*., Growth rates of large and small Southern Ocean diatoms in relation to availability of iron in natural seawater. *Limnol. Oceanogr.*, 2001, **46**(2), 260–266.
37. Sunda, W. G. and Huntsman, S. A., Interrelated influence of iron, light and cell size on marine phytoplankton growth. *Nature*, 1997, **390**, 389–392.
38. Hutchins, D. A. *et al.*, Control of phytoplankton growth by iron and silicic acid availability in the subantarctic Southern Ocean: experimental results from SAZ Project. *J. Geophys. Res.*, 2001, **106**, 31559–31572.
39. Satyaprakash, S. *et al.*, Effect of high level iron enrichment on potential nitrogen uptake by marine plankton in the Southern Ocean. *Curr. Sci.*, 2010, **99**, 1400–1404.
40. Tilzer, M. M., Elbrachter, M., Gieskes, W. W. and Beese, B., Light-temperature interactions in the control of photosynthesis in Antarctic phytoplankton. *Polar Biol.*, 1986, **5**, 105–111.
41. Westwood, K. J., Griffiths, F. B., Webb, J. P. and Wright, S. W., Primary production in the Sub-Antarctic and Polar Frontal Zones south of Tasmania, Australia; SAZ-Sense survey, 2007. *Deep-Sea Res. II*, 2011, **58**, 2162–2178.
42. De Baar, H. J. W. *et al.*, Nutrient anomalies in *Fragilariopsis kerguelensis* blooms, iron deficiency and the nitrate/phosphate ratio (A.C. Redfield) of the Antarctic Ocean. *Deep-Sea Res. II*, 1997, **44**, 229–260.
43. Croot, P. L., Andersson, K., Ozturk, M. and Turner, D. R., The distribution and speciation of iron along 6 degrees east in the Southern Ocean. *Deep-Sea Res. II*, 2004, **51**, 2857–2879.
44. Mengelt, C. *et al.*, Phytoplankton pigment distribution in relation to silicic acid, iron and the physical structure across the Antarctic Polar Front, 1701W, during austral summer. *Deep-Sea Res. II*, 2001, **48**, 4081–4100.

ACKNOWLEDGEMENTS. We thank the Ministry of Earth Sciences, Government of India for providing financial support; and the Director, NCAOR, Goa for providing the necessary facilities and support for this work. We also thank Dr C. T. Achuthankutty and Dr K. P. Krishnan for help while conducting on-board experiments and providing constructive comments; C. K. Haridevi for helping in recalculating the PP values, and the captain, officers and crew members of *ORV Sagar Nidhi* for their assistance during on-board sampling. This is NCAOR contribution number 15/2014.

Received 1 November 2013; revised accepted 8 July 2014